Available online at www.sciencedirect.com
ScienceDirect
Polymer 49 (2008) 225–233
polymer
www.elsevier.com/locate/polymer

Electrochemical synthesis and characterization of novel bile acid functionalized polypyrroles

Yan Li [a,b], Weixia Zhang [a], Guangtao Li [a,*], Yong Ju [b,**]

[a] Key Lab of Organic Optoelectronics and Molecular Engineering, Department of Chemistry, Tsinghua University, Beijing, 100084, China
[b] Key Laboratory of Bioorganic Phosphorus Chemistry and Chemical Biology, Department of Chemistry, Tsinghua University, Beijing, 100084, China

Received 12 September 2007; received in revised form 1 November 2007; accepted 4 November 2007
Available online 3 December 2007

Abstract

A new series of pyrroles bearing bile acid moieties were synthesized and electrochemically polymerized in acetonitrile with tetrabutylammonium hexafluorophosphate ($TBAFP_6$) as the supporting electrolyte. It is found that these functionalized monomers could form polypyrrole films, but their electrochemical properties and the stability of the films are strongly dependent on the length of the alkyl spacer between pyrrole ring and the pendant bile acid moiety. Each of the resulting polymers with different bile acid groups shows a distinctive behaviour in terms of its microstructure of surface, as well as electrochemical and optical properties. Compared to other analogous polypyrroles, the optical property of the cholic acid functionalized polymer is sensitive to the polarity of the used solvents, exhibiting solvatochromic behaviour. This phenomenon is probably derived from its unique facial amphiphilic structure.

Keywords: Bile acid; Conjugated polymer; Electrochemistry

1. Introduction

Bile acid is a class of natural origin steroidal compounds and plays a very important role in biological systems [1]. In the past years, bile acids and their derivatives have been extensively explored for pharmacological applications [2]. Besides its biological importance, it is well recognized that such molecules are useful components for the construction of functional supramolecular systems [3]. It is especially true for the case of cholic acid, which is one of the primary bile acids found in human and a rare naturally occurring molecule exhibiting facial amphiphilicity [3]. This molecule has a rigid concave of hydrophobic backbone and a hydrophilic face pointing to the opposite direction through disposition of three hydroxyl groups. This unqiue contrafacial amphiphilic feature makes cholic acid conformationally sensitive to environmental conditions and as an ''ideal'' solvent-induced responsive molecule [4].

The interesting properties of bile acids and their derivatives have also prompted researchers to use these compounds in the design of new polymeric materials. The synthesis of bile acids derived polymers was first demonstrated in 1988 [5], followed by a lot of contributions by Zhu and Nichifor [6] and Zhu et al. [7], due to important biomedical applications. These polymers are expected to preserve some properties of bile acids, such as facial amphiphilicity, biocompatibility, capacity of self-assembling and high chemical stability of the steroid nucleus, exhibiting great promise for drug delivery and biomedical engineering applications [6]. So far, however, most of the bile acid polymers synthesized rely on the radical polymerization of methacryloyl group or the direct condensation between carbonyl and hydroxyl groups. The residue of initiator and coupling agents may not be tolerated or even toxic for biosystems [8].

Conductive polymers (CPs) have been the subject of intense research and development because of their academic interest and tremendous technological applications [9].

* Corresponding author. Tel./fax: +86 10 62792905.
** Corresponding author. Tel.: +86 10 62792795.
E-mail addresses: lgt@mail.tsinghua.edu.cn (G. Li), juyong@tsinghua.edu.cn (Y. Ju).

0032-3861/$ - see front matter © 2007 Elsevier Ltd. All rights reserved.
doi:10.1016/j.polymer.2007.11.010

Electrodeposition of conducting polymers offers a simple and attractive approach for preparing functional materials [10]. Among conducting polymers, polypyrrole is the most thoroughly studied and applied due to its ease of modification, excellent environmental stability and relatively low oxidation potential [11]. It has been reported that the homopolymerization of cholesterol functionalized pyrrole derivatives has been achieved in CH_3CN solution [12], whereas has failed for thiophene analogues [13]. In addition, polypyrrole derivatives exhibit some unique advantages for potential medical applications because of their excellent electrical properties and biocompatibility [14,15]. The facial amphiphilic nature of bile acid could allow the polypyrrole matrix to interact favorably with the biological environment, thus enhancing its biocompatibility.

In this respect, we are interested in exploring the electrochemical oxidation as new synthetic utility for the construction of novel bile acid functionalized macromolecules. In this work, the synthesis of new *N*-substituted pyrrole derivatives bearing cholic, deoxycholic and dehydrocholic acid moieties as well as their electropolymerization was demonstrated. The resulting polymers were characterized by CV, water contact angle, microscopy and spectral methods. We also found that the cholic acid functionalized polypyrrole is sensitive to polarity of the used solvents, exhibiting modest solvatochromic behaviour. To the best of our knowledge, our work is the first report on the bile acid derived conjugated polymers.

2. Experimental

2.1. Materials

Tetrabutylammonium hexafluorophosphate ($TBAPF_6$), cholic acid, deoxycholic acid, dehydrocholic acid, phthalimide potassium, 1,10-dibromodecane and 1,4-dibromobutane are purchased from Sigma Company and were used without further purification. Pyrrole and other solvents were received from Beijing Chemicals Company and purified according to standard procedures. The synthetic protocols of *N*-(10-bromodecyl)pyrrole [16] and *N*-(10-aminodecyl)pyrrole [17] were adapted from published reports.

2.2. Characterization

IR spectra were recorded on AVATAR 360 ESP FTS spectrophotometer with KBr pellets. ^{1}H NMR spectra were recorded at 300 MHz for protons on JOEL JNM-ECA300 spectrometer. Chemical shifts (δ) are given in ppm relative to TMS ($\delta = 0.0$). The HRMS (ESI) was measured on Bruker APEX spectrometer in positive mode. SEM experiments were performed with JEOL-6301F scanning electron microscope. Contact angles were measured with a Dataphysics contact angle system. The roughness parameter Rms was determined by AFM, using SPA-400 scanning probe in dynamic force mode. The perspective view is 10 μm × 10 μm. UV–vis characterization was carried out on a Perkin–Elmer Lambda35 spectrometer. The electropolymerization was carried out with a HEKA PG310 potentiostat (Dr. Schulz GmbH, Germany) in a three-electrode single-compartment cell. The working electrode was button platinum sealed in a Teflon holder with a surface of 4 mm^2 and was polished with Al_2O_3 polishing paste prior to use. The counter electrode is a platinum wire, and a saturated Ag/AgCl electrode was chosen as reference electrode.

2.3. Synthesis of pyrrole monomers bearing bile acid moieties

2.3.1. N-[10-(3α, 7α, 12α-trihydroxy-5β-cholan)decyl]-pyrrole (**4a**)

Cholic acid (0.816 g, 2.0 mmol), DCC (0.794 g, 2.2 mmol) and HOBt (0.297 g, 2.2 mmol) were dissolved in 6 ml dry DMF. After 10 min stirring at 0 °C, compound **3a** (0.475 g, 1.9 mmol) was added and the resulting reaction mixture was kept at ambient temperature for further 20 h. After separated from precipitate, the solution was poured into 30 ml ethyl acetate. The filtrate was washed with brine and dried over $MgSO_4$. The crude product was purified on silica gel, using CH_2Cl_2/CH_3OH (30:1 to 15:1) as eluent. Concentration of the product-containing fractions gave a white solid (755.8 mg) in 65% yield. Amorphous white powder. IR (KBr): 3394.7, 2925.9, 2853.1, 1646.8, 1465.6, 719.9 cm^{-1}. ^{1}H NMR ($CDCl_3$): $\delta = 6.64$ (t, 2H, pyrrole), 6.13 (t, 2H, pyrrole), 5.81 (br, s, 1H, NH), 3.97 (br, s, 1H, 12α-CH), 3.72 (m, 3H, 7α-CH, NHCH_2), 3.44 (br, s, 1H, 3α-CH), 3.21 (m, 2H, NCH_2), 1.10–2.32 (m, 40 H, aliphatic H), 1.00 (d, 3H, 21-CH_3), 0.89 (s, 3 H, 19-CH_3), 0.68 (s, 3H, 18-CH_3). HRMS (ESI) found: 630.5214, $[C_{38}H_{64}N_2O_4 + NH_4]^+$ calcd: 630.5210.

2.3.2. N-[10-(3α, 12α-dihydroxy-5β-deoxycholan)decyl]-pyrrole (**5a**)

This compound was synthesized using the same procedure as described for **4a**, with deoxycholic acid instead of cholic acid.

Yield: 67%. Amorphous white powder. IR (KBr): 3385.0, 2927.0, 2825.0, 1647.2, 1553.9, 1043.6, 719.6 cm^{-1}. ^{1}H NMR ($CDCl_3$): $\delta = 6.64$ (t, 2H, pyrrole), 6.12 (t, 2H, pyrrole), 5.56 (br, s, 1H, NH), 3.96 (br, s, 1 H, 12α-CH), 3.74 (t, 2H, NHCH_2), 3.58 (br, s, 1H, 3α-CH), 3.22 (m, 2H, NCH_2), 1.25–2.26 (m, 42H, aliphatic H), 0.97 (d, 3H, 21-CH_3), 0.90 (s, 3H, 19-CH_3), 0.67 (s, 3H, 18-CH_3). HRMS (ESI) found: 614.5263, $[C_{38}H_{64}N_2O_3 + NH_4]^+$ calcd: 614.5261.

2.3.3. N-[10-(3α, 7α, 12α-trioxo-5β-dehydrocholan)decyl]-pyrrole (**6a**)

This compound was synthesized using the same procedure as described for **4a**, with dehydrocholic acid instead of cholic acid. Yield: 70%. White solid. IR (KBr): 3292.6, 2926.4, 2853.1, 1723.4, 1706.9, 1738.4, 1279.3, 839.7, 724.1 cm^{-1}. ^{1}H NMR ($CDCl_3$): $\delta = 6.57$ (t, 2H, pyrrole), 6.05 (t, 2H, pyrrole), 5.56 (br, s, 1H, NH), 3.79 (t, 2H, NHCH_2), 3.15 (m, 2H, NCH_2), 1.06–2.90 (m, 43H, aliphatic H), 0.10 (s, 3H, 18-CH_3), 0.77 (d, 3H, 21-CH_3). HRMS (ESI) found: 624.4747, $[C_{38}H_{58}N_2O_4 + NH_4]^+$ calcd: 624.4740.

*2.3.4. N-[4-(3α, 7α, 12α-trihydroxy-5β-cholan)butyl]-pyrrole (**4b**)*

This compound was synthesized using the same procedure as described for **4a**, with **3b** instead of **3a**. Yield: 64%. Amorphous white powder. IR (KBr): 3430.4, 2928.4, 1646.3, 845.2, 721.4, 557.9 cm^{-1}. ^1H NMR ($CDCl_3$): $\delta = 6.63-6.66$ (t, 2H, pyrrole), 6.12–6.13 (t, 2H, pyrrole), 5.90–5.93 (br, s, 1H, NH), 3.96 (br, s, 1 H, 12α-CH), 3.83–3.88 (m, 3H, 7α-CH, $NHCH_2$), 3.41–3.48 (br, s, 1H, 3α-CH), 3.19–3.27 (m, 2H, NCH_2), 2.02–2.45 (m, 6H, $NHCH_2CH_2$, NCH_2CH_2, 23-CH_2), 1.10–1.95 (m, 22H, aliphatic H), 0.96 (d, 3H, 21-CH_3), 0.90 (s, 3H, 19-CH_3), 0.74 (s, 3H, 18-CH_3). HRMS (ESI) found: 546.4266, $[C_{32}H_{52}N_2N_2O_4 + NH_4]^+$ calcd: 546.4271.

2.4. General procedure for electrosynthesis of the polypyrrole films bearing bile acid units

The oxidation potentials of the synthesized pyrrole monomers were determined in a 1×10^{-3} M acetonitrile solution containing 0.1 M $TBAPF_6$ as supporting electrolyte. For polymerization process, 60 mM of the corresponding monomer was used and electropolymerized by repetitive cyclic scanning in a potential range. The resulting electroactive polymers were rinsed with acetonitrile and characterized in an electrolyte solution free of monomer. In all cases, experiments have been carried out under N_2 atmosphere at room temperature. Indium tin oxide (ITO, 2×1 cm^2) glass was used as working electrode to produce thin-film coatings of bile acids derived polypyrrole for the characterization of morphology and optical properties as well as for IR measurements. A polymeric film had been deposited on the ITO glass electrode after 20 cycles and washed carefully with acetonitrile then dried in vacuum for further characterization.

2.5. Optical characterization of bile acid functionalized polymer films

Polymer-coated ITO glass slice was vertically placed in a cuvette containing a mixed solvent of $CHCl_3$ and CH_3OH with different ratios for 20 s, in such a way to ensure the change of the steroid conformation without destroying the conductive polymer layer on ITO glass. In all cases, the polypyrrole films were used in the neutral form and a bare ITO glass in the corresponding solvents was used as reference for UV–vis study.

3. Results and discussion

3.1. Synthesis and electropolymerization

Scheme 1 displays the synthetic route of a series of *N*-substituted pyrrole derivatives with pendant bile acid moieties. The synthesis started with an alkaline-mediated coupling reaction of α,ω-dibromoalkane (1,10-dibromodecane or 1,4-dibromobutane) with pyrrole [16]. Subsequently, using Gabriel synthesis, the resulting bromide was transformed into terminal amino group by the reaction with potassium phthalimide followed by hydrazinolysis [17]. Direct condensation of bile

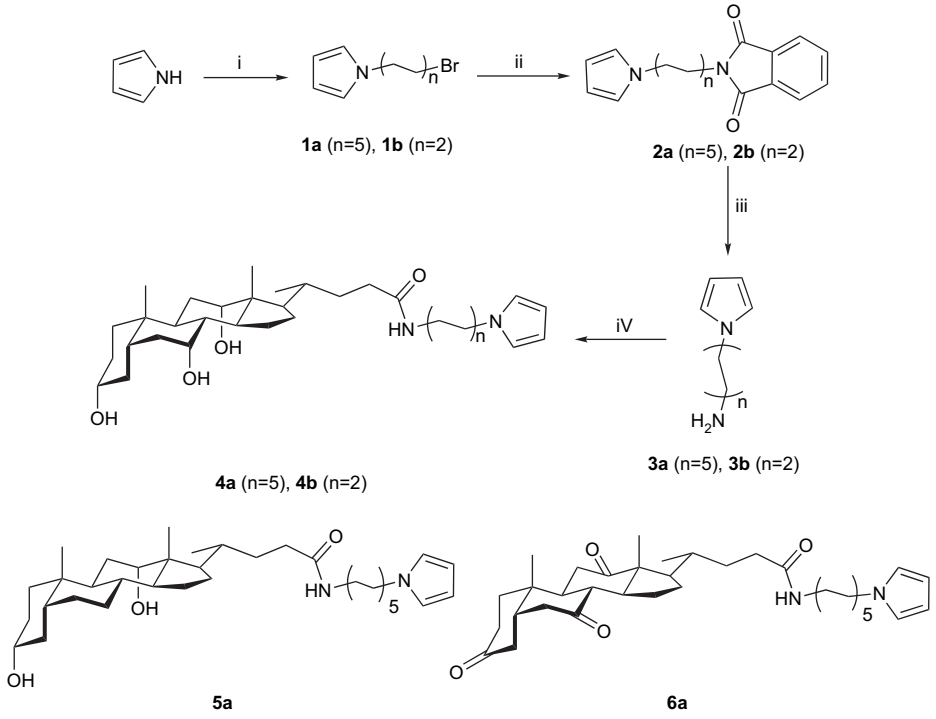

Scheme 1. Synthesis of *N*-substituted pyrrole derivatives with pendant bile acid moieties. Reagents and conditions: (i) $Br(CH_2)_nBr$, NaH, DMF, r.t. 3 h and 70% yield; (ii) phthalimide potassium, DMF, reflux, 24 h; (iii) (a) N_2H_4/ethanol, reflux, 24 h; (b) KOH/H_2O; (iv) DCC/HOBt, cholic acid, DMF, 20 h; (v) DCC/HOBt, deoxycholic acid, DMF, 20 h; (vi) DCC/HOBt, dehydrocholic acid, DMF, 20 h.

Table 1
Oxidation potentials of the monomers and the resulting homopolymers

Monomer	E^{oxd} (V)	Polymer	E^{oxd} (V)	E^{red} (V)
4a	1.19	**P4a**	1.14	0.87
5a	1.18	**P5a**	0.98	0.85
6a	1.16	**P6a**	0.88	0.81
4b	1.19	**P4b**	>0.8	>0.8
1b	1.13	**P1b**	0.45	0.42

acid with amine group, using DCC in the presence of HOBt, afforded title compounds in fine isolated yield. The obtained new pyrrole monomers are characterized by three different bile acid groups (dehydrocholic, deoxycholic and cholic acid) and two different alkyl spacers between the pyrrole ring and the pendant functional units.

The oxidation potentials of the new functionalized pyrrole monomers were determined by means of CV in acetonitrile solution containing 0.1 M $TBAPF_6$ as supporting electrolyte. Low monomer concentration (1 mM) was used in order to detect the occurrence of polymerization. As expected, these monomers exhibit an irreversible oxidation wave centered at about 1.2 V (vs Ag/AgCl) in their CVs. Since the functional groups in the bile acids (hydroxyl and amide) are electrochemically inert under the used conditions, the observed redox process is fully due to the oxidation of the pyrrole ring. Table 1 lists the measured oxidation potentials. For the sake of comparison, the oxidation potential of *N*-(10-bromodecyl)pyrrole is also displayed in Table 1. Obviously, the new monomers show nearly the same potential, comparable to the potential of other *N*-alkyl pyrroles. This result indicates that the four methylene units are long enough to fully decouple the electronic effect of the bulky steroid groups on the pyrrole ring system.

The electropolymerization was accomplished in a CH_3CN/$TBAPF_6$ medium by repeated potential cycling over the range of 0–1.5 V. Fig. 1a–d displays the potentiodynamic polymerization process of the monomers **4a**, **5a**, **6a** and **4b**, respectively. As typical for polypyrrole, upon successive potential scans, both anodic and cathodic waves in a potential lower than the oxidation potential of the corresponding monomer occurred, pointing out that a new redox material emerged on the electrode surface. In the case of the monomers **4a**, **5a** and **6a**, the steady increase of the redox wave with scan cycles indicates that the conductivities of the deposited polymers are

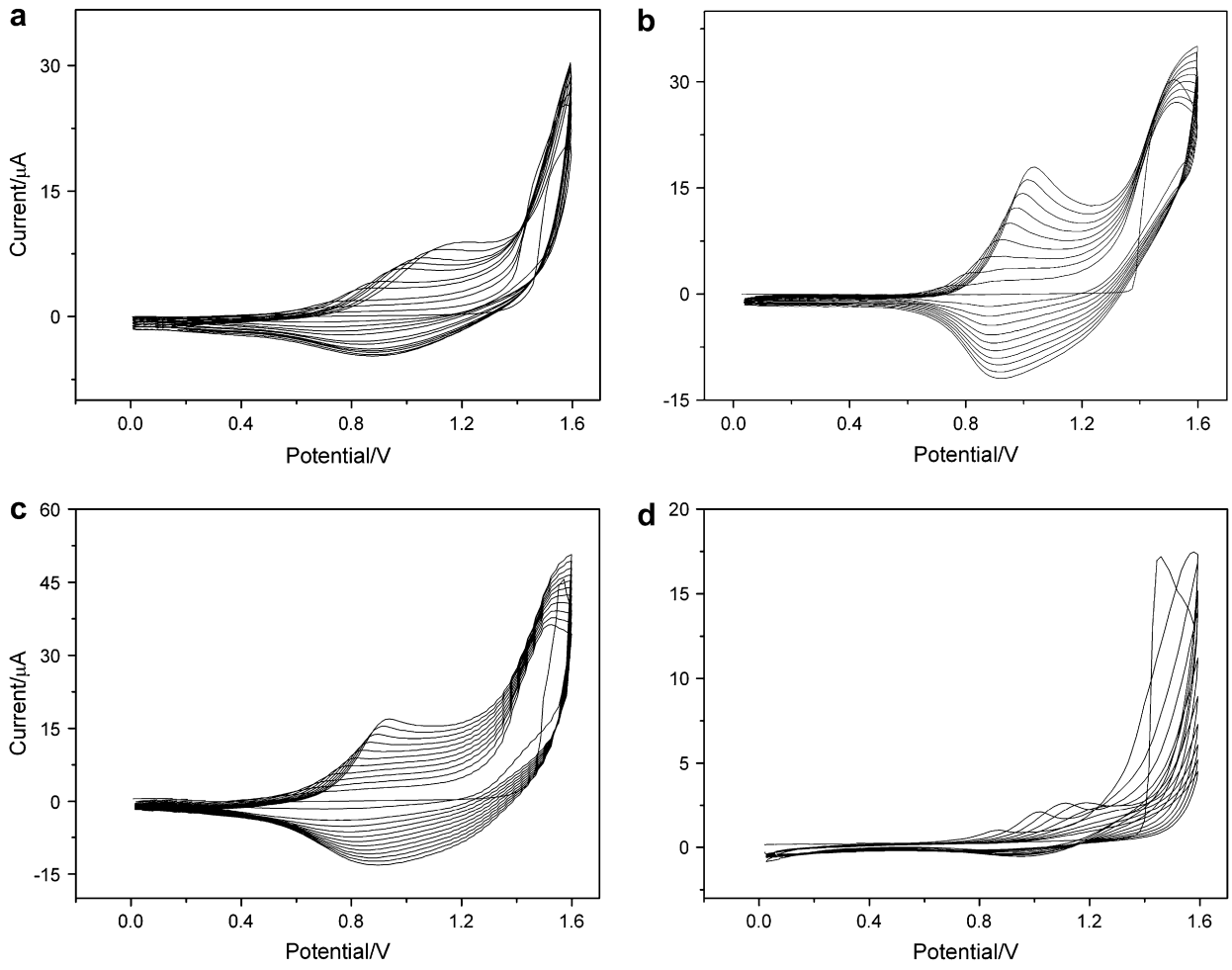

Fig. 1. Repetitive cyclic voltammogram of 60 mM (a) **4a**; (b) **5a**; (c) **6a** and (d) **4b** in $TBAFP_6$–CH_3CN solution using a 4 mm^2 Pt electrode at a potential scan rate of $v = 100$ mV s^{-1}.

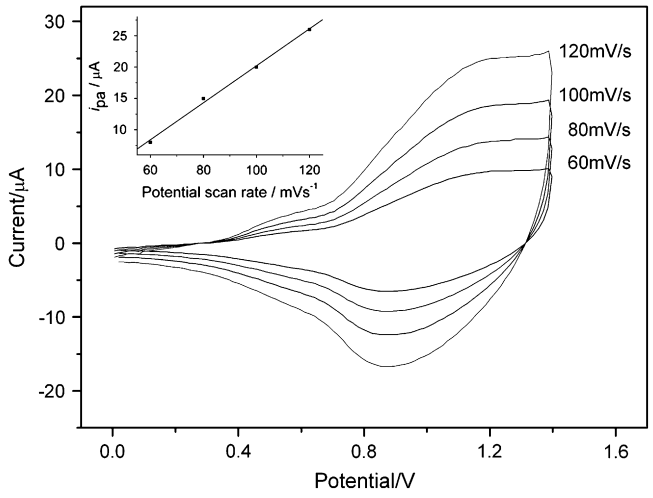

Fig. 2. CVs of **P4a** in 0.1 M $TBAPF_6$–CH_3CN solution at different scan rates. The inset shows the plot of scan speed vs anodic current, i_{pa}, for a Pt disk electrode coated with **P4a**.

high enough to sustain polymer growth. The oxidation waves are substantially more positive than typical *N*-substituted pyrroles due to steric factor [18]. Compared to its analogous compounds **5a** and **6a**, it was evident that the oxidation potential of **4a** increased significantly in the course of polymerization, suggesting the poorer surface conductivity, which results from the extra steric hindrance and insufficient packing interfered by the three hydroxyl groups on the backbone.

Construction of conjugated π-electron structure that can efficiently ''feel'' the conformational change of bile acid is our desired system. Unfortunately, the analogues **4b** with a shorter alkyl spacer exhibits poor polymerizability. As demonstrated in Fig. 1d, the first voltammogram of **4b** did show the anodic current cross-over feature associated with polymer nucleation at the electrode surface. After the increase of redox waves in initial few cycles, however, the intensity of current decreased dramatically in subsequent scans and the electrode surface slowly became passivated. The above-described results show that reducing the distance between pyrrole ring and bile acid unit to promote the interaction will give rise to considerable crowd of bulky and rigid steroid moieties, thereby resulting in short efficient conjugation length and poor conductivity. In addition, because of the large steric hindrance, the successful polymerization of all these monomers requires a higher concentration (60 mM) than other reported typical *N*-substituted pyrroles [15,18].

3.2. Characterization by CV

After the polymerization, the deposited polymers were carefully rinsed with acetonitrile and characterized at different scan rate in an electrolyte solution free of monomer. In Fig. 2, the voltammograms of the polymer **P4a** are displayed, which show the typical reversible redox wave of conjugated polyheterocycles. The reversible redox transition occurred in the potential range of 0.8–1.1 V and increased with the number of hydroxyl groups on the backbone of steroid (Table 1). Since the redox potentials reflect the extension of the conjugated π-electron system, these new polymers possess relatively twisted backbone and shorter conjugation lengths compared to other reported *N*-substituted polypyrroles because of the disruption by the large bile acid side groups. Both anodic and cathodic peak currents change linearly with the scan rates, indicating that the redox active species of the polymers were fixed onto the electrode surface and the related electrochemical reactions are not limited by diffusion [17,19]. As typical for conjugated polypyrrole, these polymers exhibit electrochromism (dark brown colored layers in the neutral form and green blue colored layers in the oxidized form) during the doping–dedoping process.

The films of **P4a**–**P6a** possess good stability during the oxidation–reduction process. For **P4a**, after a small loss (2–5%) of electroactivity in first several scan cycles, no appreciable changes were observed in the following scans (Fig. 3a). It is very difficult for monomer **4b** with shorter spacer to form homogeneous film on large Pt disk or ITO glass electrode. As shown in Fig. 3b, significant loss of current intensity was detected during the doping–dedoping process and this polymer

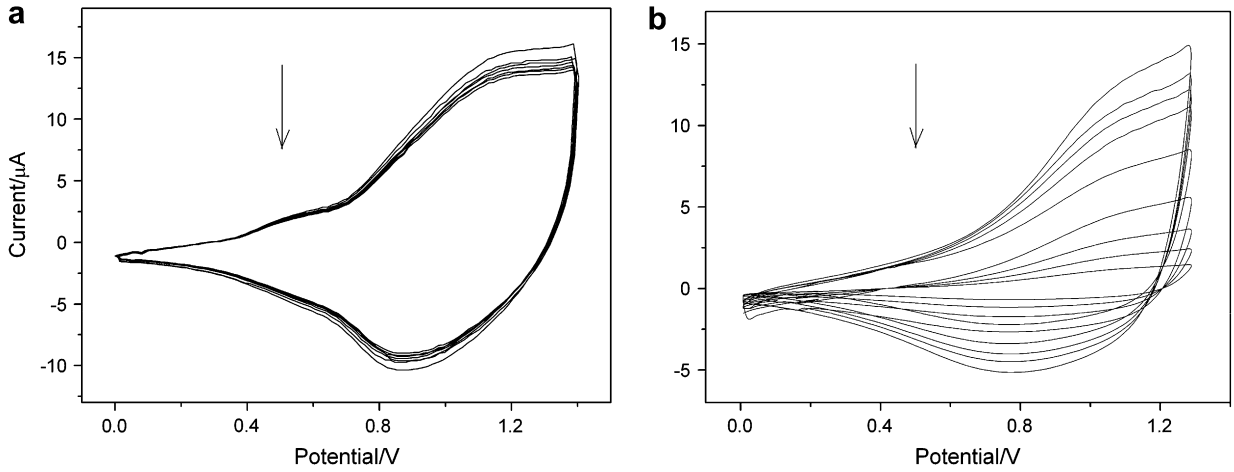

Fig. 3. Characterization of the polymer films (a) **P4a** and (b) **P4b** by repeat cyclic voltammograms.

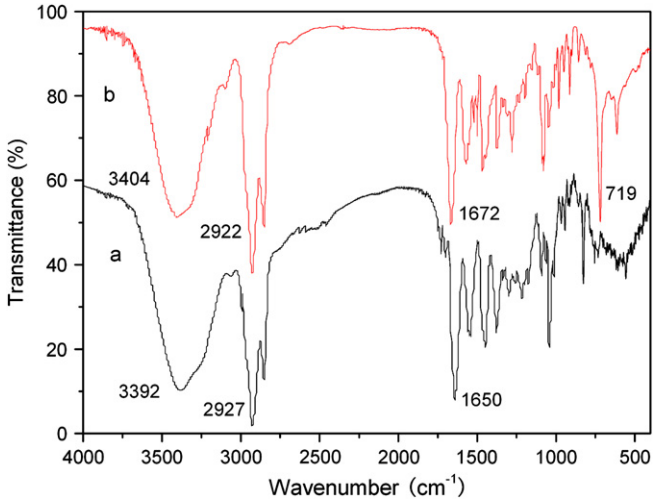

Fig. 4. (a) FT-IR spectrum of **P4a** electroformed using the CV method and (b) FT-IR spectrum of **4a**. Both spectra were acquired using KBr disk.

film almost lost its electroactivity after ten cycles. The poor stability of **P4b** was consistent with the observed phenomenon during the electropolymerization.

3.3. Characterization by FT-IR

Polymer materials removed from electrodes were dried in vacuum and characterized using FT-IR spectroscopy in neutral form. The measurements confirmed that the used bile acid units were correctly incorporated into synthesized polymers and all functional groups withstood the polymerization. The FT-IR spectrum of a **P4a** film is shown in Fig. 4a, alongside that of the monomer **4a** for comparison. It is clearly visible that an absorption of out-of-plane bending (−CH) of the pyrrole at about 720 cm^{-1} almost disappears after the polymerization, indicating the α−α coupling of pyrrole units [19]. Additionally, both the polymer and the monomer show the signals from the characteristic vibrations of methyl groups of steroid moiety at 1390 cm^{-1}, amide unit at about 1640 cm^{-1} (amide I) and 1530 cm^{-1} (amide II) as well as the broad band centered at 3380 cm^{-1} for hydroxyl groups. A slight shift of carbonyl and hydroxyl groups absorptions to lower wavelength was observed in the spectra of polymer, suggesting the presence of hydrogen bonding in the polymer matrix [20]. The similar results were also observed in the case of other polymers, indicating that the structure of bile acid was retained after the polymerization and the bile acid derived polypyrroles have been successfully coated on the electrodes.

Table 2
Surface properties of bile acid derived polypyrroles

Polymer	**P4a**	**P5a**	**P6a**
Water contact angle[a] (deg)	80 (±1)	93 (±1)	88 (±1)
Rms [b] (nm)	167	120	63

[a] The water contact angle is mean of three values on different points of one film.
[b] Rms is the root-mean-square roughness, which is defined as the standard deviation of the distribution of surface heights.

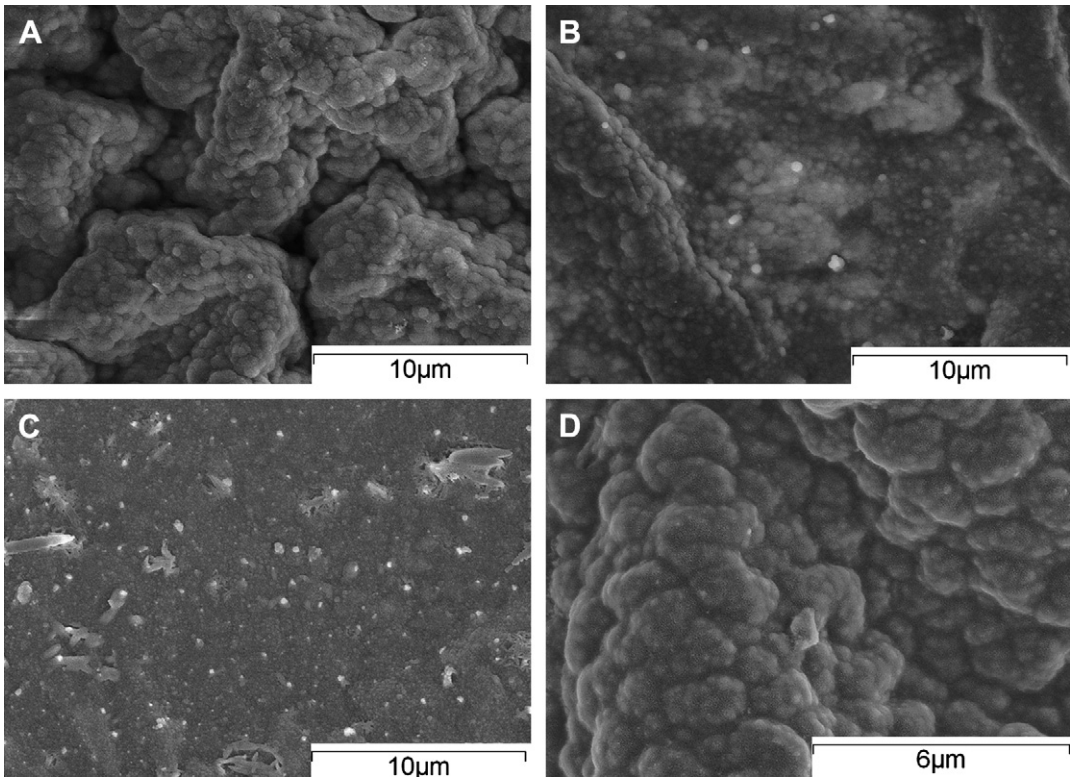

Fig. 5. SEM images of polypyrrole films: (A) **P4a**; (B) **P5a**; (C) **P6a** and (D) detailed structure of one swell on **P5a**.

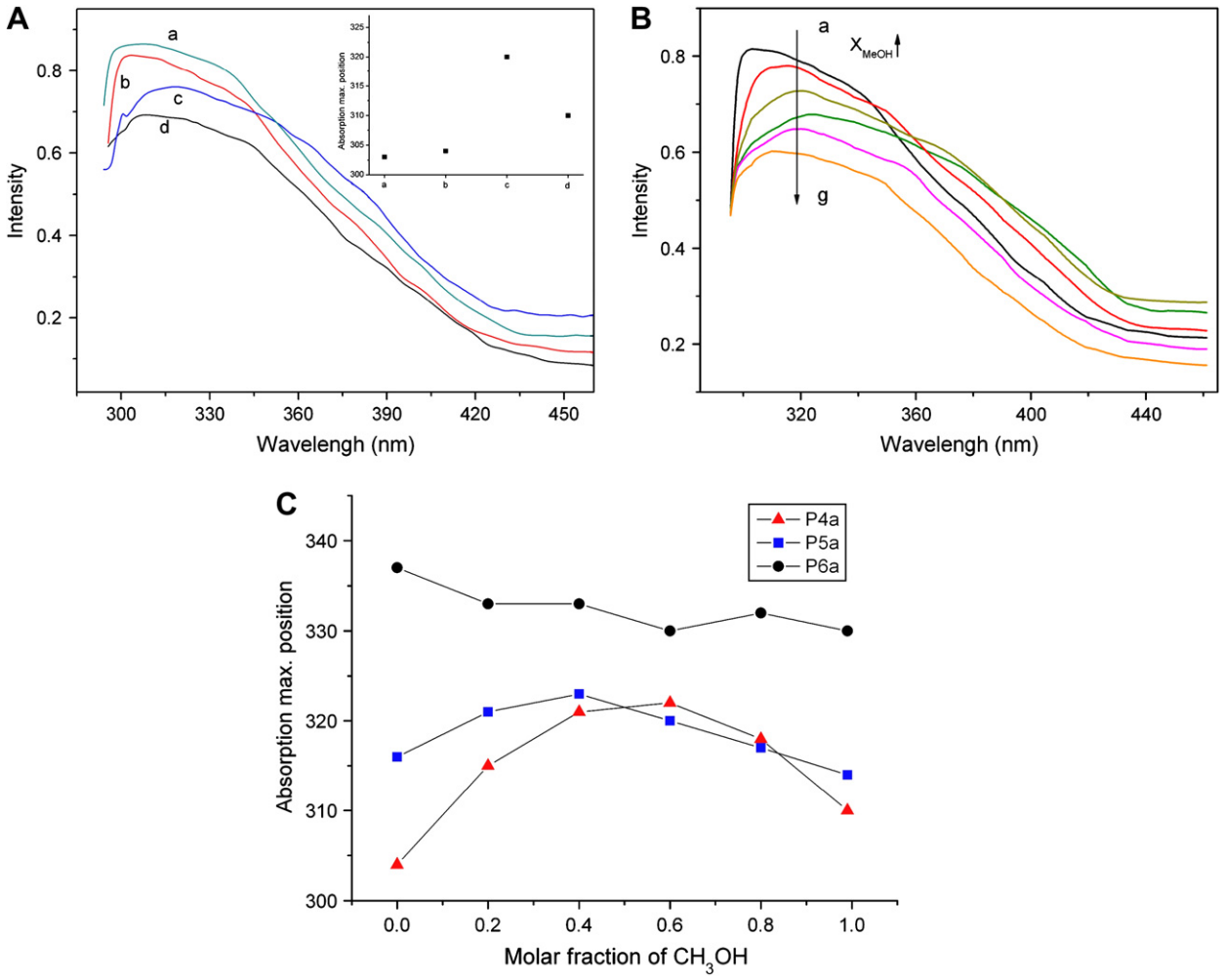

Fig. 6. (A) UV–vis absorption spectra of **P4a** film in different solvents at 20 °C: (a) cyclohexane, (b) $CHCl_3$, (c) THF, (d) CH_3OH; The inset shows the plot of maximum absorption vs different solvents (B) UV–vis absorption spectra of **P4a** film in $CHCl_3$ solution at 20 °C with the molar fraction of MeOH: (a) 0.00, (b) 0.20, (c) 0.40, (d) 0.60, (e) 0.80, (f) 0.99; (C) X_{MeOH} dependence of the maximum absorption in UV–vis spectra for **P4a**, **P5a** and **P6a**.

3.4. Characterization on surface properties

In order to obtain information about the physical properties of these conductive polymer-coated surfaces, wettability and SEM experiments were carried out. Table 2 summarizes the value of water contact angle of the polymers electrochemically formed on the ITO glass. It has been reported that the neutral polypyrrole is usually slightly hydrophilic, with the water contact angle about 48 °C [21]. Much larger values were obtained from the bile acid functionalized polypyrrole, which is consistent with the fact that bile acid moieties are hydrophobic domain [22]. However, the data in this experiment are anomalous, which did not agree with the polarity sequence of these bile acids. The contact angle of **P6a** that has the least polarity, lies well between that of **P4a** and **P5a**. Yet, the wettability of solid surfaces is governed by both the chemical composition and the geometrical microstructure of the surface [23].

Scanning electron microscope (SEM) was used to characterize the microstructure of this functionalized polypyrrole films. Fig. 5 presents the SEM images of the polymers obtained from **4a**–**6a** on ITO glass electrodes. Although special attention was paid to deposit the films in the same condition, significant differences can be observed in these polymers despite their structural similarity. It can be clearly seen that the electropolymerization of monomers **6a** gave a rather compact and homogeneous polymer surfaces, comparable to other typical *N*-substituted polypyrrole derivatives [15]. On the contrary, the other two polymers, especially **P4a**, exhibit rough and loose surfaces with many concaves and swells. The surface properties were further confirmed by AFM with perspective view of 10 μm × 10 μm. The Rms parameters are listed in Table 2. The values of **P4a** and **P5a** were much larger than **P6a**, which was consistent with the SEM images. The cholic acid and deoxycholic acid, which is composed of a bent and rigid backbone with several hydroxyl groups, are typically unfavourable to compact packing and tend to form amorphous polymers due to phase separation [24]. We believe that it is the amorphous structure and rough surface that enhances the hydrophobicity of **P5a**. In addition, this amorphous structure could also aid in sensor capabilities because of the larger surface area that will be discussed later.

3.5. Optical characterization

Like other reported electrogenerated conducting polymers, the polymer materials **P4a**–**P6a** obtained here are insoluble in common organic solvents and the determination of their molecular weight by gel permeation chromatography (GPC) failed. UV–vis experiment was carried out in solid state and the absorption maximum (λ_{max}) in the spectrum can be a criterion for the comparison of conjugation length of these polymers. The absorption spectrum of film **P4a** in the reduced form exhibits a band with a maximum at 308 nm and a shoulder at ca. 344 nm, attributable to the characteristic π–π^* interband transition [25]. The λ_{max} of deoxycholic and dehydrocholic acid derived polypyrrole is about 316 nm and 337 nm, respectively, indicating their longer effective conjugation length than cholic acid derived polypyrrole. Compared to the unsubstituted pyrrole monomer, typically $\lambda_{max} = 220$ nm, these UV–vis absorptions are indicative of a larger HOMO–LUMO "band" gap. In all cases, the absorption maximum of the prepared polymers is smaller than common polypyrrole and no absorption peak was observed above 450 nm, suggesting that the bulky bile group hinders the formation of more planar backbone conformation.

It is well known that the electrochemical and optical properties of CPs are sensitive to their environmental exposure. Any minor perturbation of the side chain leads to dramatic changes in their conductivity, electrochemical behaviour and spectroscopic properties through a unique amplification mechanism [26]. This characteristic determines CPs excellent transduction materials that readily transform a chemical signal into an easily measured optical event [27,28], even when the functional groups on the side chain are well separated from the polymer backbone. As described in Section 1, cholic acid is an "ideal" conformational responsive molecule. Attaching such functional group onto the conjugated system is expected to develop stimuli-responsive materials, in which the conformation sensitivity of cholic acid unit to solvent will immediately cause the change of the conjugation length with readable optical signal. Thus, according to the method described in Section 2, the polymers derived from cholic acid–pyrrole conjugates were characterized by UV–vis spectroscopy by dipping the coated ITO glass into solvents with different polarity (Fig. 6A). As demonstrated in Scheme 2, the cholic acid unit can form aggregation in both absolute polar and non-polar media due to its facial amphiphilic character [29]. Under such circumstances, the polymer chain may take nonplanar conformation, leading to a reduction in the effective conjugation length of the polypyrrole backbone. THF is, however, a good solvent for both hydrophilic and hydrophobic faces, in which the polypyrrole backbone takes an extended planar conformation and is better conjugated. With the progressive addition of methanol to chloroform solution, the absorption band becomes wider and the absorption maximum reaches a threshold value, corresponding to the molar fractions of MeOH (X_{MeOH}) of about 0.6 (Fig. 6B). This threshold could correspond to the highly solvating system that prevents the aggregation of the cholic acid moieties. Further additions of methanol beyond this limit

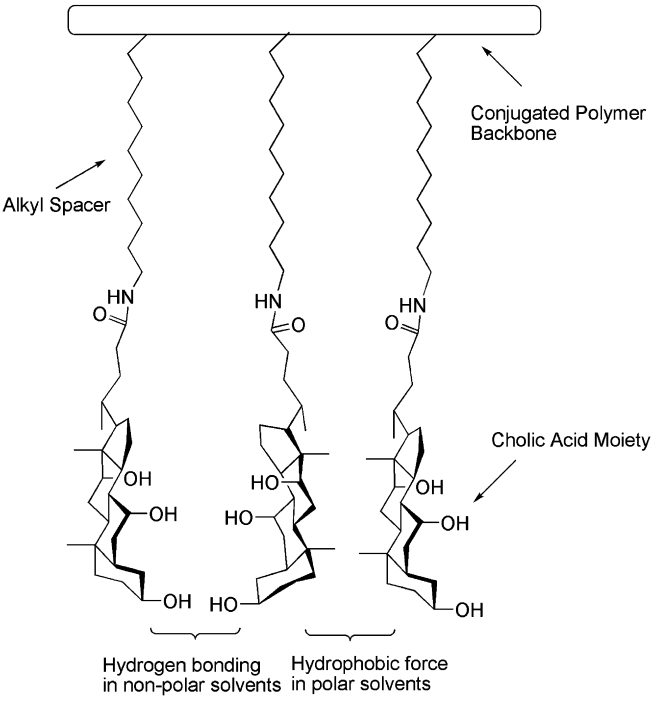

Scheme 2. The structure of cholic acid derived polypyrrole **P4a**.

lead to a slightly reverse solvatochromic behaviour of the polymer with the less conjugated form: the absorption maximum blue shifts to $\lambda = 310$ nm. Compared to **P4a**, polymer **P5a** presents much weaker solvatochromic behaviour ($\Delta\lambda_{max} \approx 11$ nm) as shown in Fig. 6C, indicating that the hydroxyl group at the position 7 plays an important role in forming intermolecular hydrogen bonding and building the amphiphilic structure [30]. For **P6a**, which the amphiphilic property was lost due to the absence of any hydroxyl group, the shift of UV–vis absorption was negligible. Similar side chain aggregation induced solvatochromic behaviour has also been reported on polyacetylene [31] and many other π-conjugated systems [32,33]. The amorphous surface of **P4a** may be helpful for such sensor capability.

Somewhat disappointingly, the overall shifts in UV spectra are rather small. This may stem from one or a combination of the following factors: (a) the long spacer which is crucial for successful polymerization considerably weakened the influence between the steroid moiety and the backbone of polypyrrole; (b) a high level of defect formation or cross-linking may be present in the polymer matrix through electropolymerization, making the structure different from the model we expected; (c) since the solvatochromic behaviours were measured in solid state and the conjugation length in polymer chains is relative short, there might not be much room for the rearrangement of the conjugated backbone.

4. Conclusions

With the synthesis of pyrrole derivatives bearing cholic, deoxycholic and dehydrocholic acid moieties, three new functionalized polypyrroles were produced by electrochemical

polymerization. Due to the rigid bulky structure of steroid moiety, the length of the spacer between bile acid and the conjugated backbone, and the extension of effective conjugation length are the two crucial factors for the construction of bile acid based functional conjugated systems. Each of the three polymers exhibits distinctive characteristics in terms of its microstructure of the surface as well as electrochemical and optical properties. It was also found that the combination of bile acid (conformational responsive molecule) and conjugated polymers (physicochemical sensitive system) leads to novel functional materials, which can sense environmental conditions (polarity of solvent) with readable optical signal. Compared to deoxycholic and dehydrocholic acid moieties, cholic acid is the best candidate for the development of the above-described system due to its remarkable facial amphiphilic feature. This is the first example of the integration of bile acid units with conjugated π-electron polymer system. Based on these preliminary results, we believe that optimization of the related factors should result in more efficient and biocompatible responsive systems, which could find applications in chemical sensor and biomedical device.

Acknowledgements

We gratefully acknowledge the financial support from the National Science Foundation of China (20473044, 20533050, 20772071, 50673048,) and 973 Program (2006CB806200).

References

[1] Sjövall J. Lipids 2004;39:703.
[2] Salunke DB, Hazra BG, Pore VS. Curr Med Chem 2006;13:813.
[3] Virtanen E, Kolehmainen E. Eur J Org Chem 2004:3385.
[4] Ryu EH, Yan J, Zhong Z, Zhao Y. J Org Chem 2006;71:7205.
[5] Ahlheim L, Hallensleben ML. Makromol Chem Rapid Commun 1988; 9:299.
[6] Zhu XX, Nichifor M. Acc Chem Res 2002;35:539.
[7] Hao JQ, Li H, Zhu XX. Biomacromolecules 2006;7:995.
[8] Gautrot JE, Zhu XX. Angew Chem Int Ed 2006;45:6872.
[9] Skotheim TA, Esenbaumer RL, Reynolds JR. Handbook of conducting polymers. 2nd ed. New York: Marcel Dekker; 1998.
[10] Roncali J. J Mater Chem 1999;9:1875.
[11] Zang Z, Roy R, Dugre JF, Tessier D, Dao HL. J Biomed Mater Res 2001;57:63.
[12] Chen Y, Imrie CT, Ryder KS. J Mater Sci Lett 2002;21:595.
[13] Irpan C, Alkan S, Toppare L. J Mater Sci 2002;37:1767.
[14] Shustak G, Gadzinowski M, Slomkowski S, Domb AJ, Mandler D. New J Chem 2007;31:163.
[15] Okner R, Domb AJ, Mandler D. Biomacromolecules 2007;8:2928.
[16] Guo RR, Li GT, Zhang WX, Shen GQ, Shen DZ. ChemPhysChem 2005; 6:2025.
[17] Li GT, Bhosale S, Tao SY, Bhosale S, Fuhrhop J. J Polym Sci Part A Polym Chem 2005;43:4547.
[18] Haddour N, Cosnier S, Gondran C. J Am Chem Soc 2005;127:5752.
[19] Chen Y, Imrie CT, Ryder KS. J Mater Chem 2001;11:990.
[20] Nasdala L, Beran A, Libowitzky E. Am J Sci 2001;301:831.
[21] Xu L, Chen W, Mulchandani A, Yan Y. Angew Chem Int Ed 2005;44:6009.
[22] Neralagatta MS, Bhat S, Choudhury AR, Maitra U, Terech P. J Phys Chem B 2004;108:16056.
[23] Lafuma A, Qumrm D. Nat Mater 2003;2:457.
[24] Zhang JH, Bazuin CG, Freiberg S, Brisse F, Zhu XX. Polymer 2005;46: 7266.
[25] Roncali J. Chem Rev 1992;92:711.
[26] McQuade DT, Pullen AE, Swager TM. Chem Rev 2000;100:2537.
[27] Thomas SW, Joly GD, Swager TM. Chem Rev 2007;107:1339.
[28] Sandstedt CA, Rieke RD, Eckhardt CJ. Chem Mater 1995;7:1057.
[29] Ghosh S, Maitra U. Org Lett 2006;8:399.
[30] Willemen HM, Vermonden TA, Marcelis TM, Sudhölter EJR. Eur J Org Chem 2001:2329.
[31] Cheuk KKL, Lam JWY, Li BS, Xie Y, Tang BZ. Macromolecules 2007;40:2633.
[32] Dufresne G, Bouchard J, Belletete M, Durocher G, Leclerc M. Macromolecules 2000;33:8252.
[33] Erdogan B, Wilson JN, Bunz UHF. Macromolecules 2002;35:7863.